2002-01-1699

Mutagenic Potential of Particulate Matter from Diesel Engine Operation on Fischer-Tropsch Fuel as a Function of Engine Operating Conditions and Particle Size

Michael H. McMillian
National Energy Technology Laboratory

Mingzhen Cui and Mridul Gautam
West Virginia University

Michael Keane, Tong-man Ong, and William Wallace
National Institute for Occupational Safety and Health

Edward Robey
Parsons Corporation

ABSTRACT

Further growth of diesel engines in the light-duty and heavy-duty vehicular market is closely linked to the potential health risks of diesel exhaust. The California Air Resources Board and the Office of Environmental Health Hazard Assessment have identified diesel exhaust as a toxic air contaminant. The International Agency for Research on Cancer concluded that diesel particulate is a probable human carcinogen [1]. Cleaner burning liquid fuels, such as those derived from natural gas via the Fischer-Tropsch (FT) process, offer a potentially economically viable alternative to standard diesel fuel while providing reduced particulate emissions. Further understanding of FT operation may be realized by investigating the differences in toxicity and potential health effects between particulate matter(PM) derived from FT fuel and that derived from standard Federal diesel No. 2 (DF). The present effort investigates the mutagenicity of particulate matter derived from FT and DF fuel combustion in a single-cylinder diesel engine by relating the in-vitro mutagenic activity of the PM to engine operating conditions and particle size. Total particulate matter samples were gathered using glass fiber filters in a mini-dilution tunnel from engine operation on each fuel at seven steady state engine operating conditions. Particulate matter samples from two engine conditions were also gathered on greased aluminum foil substrates using a Micro-Orifice Uniform Deposition Impactor (MOUDI) for size selective mutagenic analysis using the Ames Typhimurium bioassay method. Toxicity effects are reported but screened from the dose-response analysis using a method similar to that set forth by Bernstein [2]. Results indicate mutagenic response differences in the particulate matter as functions of engine operating conditions, fuel type and particle size. Large particles exhibit a significantly greater mutagenic effect than their smaller counterparts.

INTRODUCTION

Further growth of diesel engines in the light-duty and heavy-duty vehicular market has continued to focus attention on the health risks of diesel exhaust. From a regulatory perspective, particulate matter (PM) in diesel engines is undesirable. The California Air Resources Board and the Office of Environmental Health Hazard Assessment classified Diesel Exhaust as a "Toxic Air contaminant". The International Agency for Research on Cancer concluded in 1989 that diesel particulate is a probable human carcinogen [1] while the National Institute for Occupational Safety and Health (NIOSH) concluded that it is a potential occupational carcinogen [3]. The soluble organic fraction (SOF) constituents, particularly the polynuclear aromatic hydrocarbons (PAH) and the nitro-PAH are strong contributors to the overall mutagenicity [4]. There have been several studies relating genotoxic and mutagenic potential to engine operation with standard or near standard variants of Federal Diesel No. 2 fuels [5,6,7]. However, the effects of FT fuel operation or particles size effects remain relatively unstudied. Even as regulations continue to tighten, the market portion of diesel engines in transportation applications continues to grow in overseas markets. The concerns of diesel emissions require an in-depth knowledge of their composition, their health effects, and the effect of fuel formulation on particulate emissions.

Diesel engines emit low levels of hydrocarbons and carbon monoxide that do not require aftertreatment to comply with current standards. Diesel engines also enjoy 25% to 40% higher thermal efficiency over their gasoline fueled counterparts [8]. It is however, very difficult for

diesel engines to simultaneously meet NO_x and particulate matter emissions standards. Further, NO_x and PM catalytic exhaust aftertreatment technologies have been hampered by the high sulfur content in commercially available diesel fuels.

Fuel reformulation has been used as a pollution control technique and continues to be considered as a highly effective enabling technology for emissions benefits in future transportation applications. Significant reformulation of diesel fuel (<15 ppm sulfur) has been legislated to enable aftertreatment technologies so that heavy-duty engines can meet 2007 and beyond emission regulations [9]. Market penetration of light-duty diesels has the potential for a significant impact on CO_2 emissions and a reduction in demand for imported crude oil due to offsets in overall thermal efficiency. In this regard, Fischer-Tropsch (FT) fuel is attractive due to its low sulfur content, low C/H ratio and because it may be derived from natural gas or coal thus offering future economic and strategic alternatives to U.S. oil importation.

Fischer-Tropsch (FT) fuels are made by first reforming a hydrocarbon fuel by partial combustion with steam to form a gas rich in hydrogen and carbon monoxide. The gas stream is then introduced to a reactor where catalysts promote reactions to form highly paraffinic (C_nH_{2n+2}) fuels. FT fuels have high cetane number, low aromatics, low C/H ratio and relatively low specific gravity. Their value in reducing regulated emissions in diesel engines has been demonstrated [10,11,12,13].

FT fuels are a strong candidate for fuel blending and for use as a neat fuel in future transportation markets. Their impact on aftertreatment catalyst development due to their low sulfur content and their potential to reduce diesel engine particulate emissions are attractive. Further, benefits of FT emissions reduction may be realized with a better understanding of the differences in bioactivity between particulate matter derived from F-T fuel and that derived from typical diesel fuel.

This study investigated the mutagenic activity of particulate matter derived from FT fuel combustion in a single-cylinder diesel engine as functions of engine operation and particle size. Particulate samples were gathered at seven optimized steady-state operating conditions (key states) for both Federal diesel No. 2 and the FT fuel. The term "optimized" is used here to mean that the engine was optimized for maximum thermal efficiency by adjusting fuel injection timing at constant speed and torque at each key operating state.

The extracted soluble organic fraction (SOF) of the diesel particulate matter (DPM) is analyzed using the a variant of the Ames method [14,15]. The results are used to associate mutagenic activity with engine test conditions and compare standard No. 2 diesel with FT fuels at these conditions. Also, a Micro-orifice Uniform Deposition Impactor (MOUDI) was used to collect size selective PM samples for size dependent Ames bioassay analysis at two steady-state engine operating conditions (key states). Two size-fractionated samples were collected during engine operation at key states 2 and 4 (representing low speed-low load and intermediate speed-high load conditions respectively) for each fuel type; thereby, producing a total of twelve samples for size-dependent Ames analysis. In all cases, mutagenic potential of size-fractionated PM samples were determined using a preincubation variant of the Ames Salmonella microsomal assay system [15]. The samples were tested on both YG1024 and YG1029 bacterial tester strains in the presence and absence of 10% concentration of S9, a preparation made from the livers of laboratory rats induced with Aroclor 1254. Using both strains accounted for both frameshift and basepair substitution types of mutation. The S9 demonstrates whether the mutagens cause genetic damage directly or whether they require activation by metabolic enzymes produced in mammalian livers. Concentration (dosage) ranges in the bioassays were varied from very low dosages to, in some cases, levels in which toxicity effects were apparent. Experiments were performed using four replicates, and dose-adjustment confirmation tests were run and repeated as necessary for each sample. Known mutagens and the solvent dichloromethane (DCM) were used as positive controls and the dispersants, dimethyl sulfoxide (DMSO) and Tween 80, were used as negative controls. The numbers of revertants were determined by using an automatic counter. The average number and standard deviations of revertants per plate were then determined. The revertant activity was related to initial particulate mass and engine output by carefully tracking the solvent and particulate concentrations.

In the Ames test, the relationship between revertant count and dosage was used to develop a measure of mutagenicity. For small dosages, the mean revertant count was typically assumed to be a linear function of the dose of a mutagenic substance. Further, the slope of the line relating revertant count to dose was a measure of the mutagenicity of the substance. However, at large doses, Salmonella death began to dominate due to DPM sample extract toxicity. This effectively reduced the revertant count and reduced the slope of the revertant-vs-dose curve. If revertant count data from cases exhibiting toxicity were included in the analysis to determine mutagenicty, the slopes, and hence the mutagenicity measure, would be biased downward. Toxicity effects were removed using the statistical method of Bernstein [2]in which a full data set of dose response slopes were compared with successively reduced data sets with the largest remaining dose removed. This process was repeated until no toxicity effects were indicated or until there were only three remaining doses. Bernstein [2] also recommend additional statistical tests on revertant count data sets. One of those was a test for mutagenic effect in which the null-hypothesis of no mutagenic effect (i.e. the mean revertant count was a constant that was independent of dosage, $b_1=0$) versus the alternative that

the mean revertant count was a linear function of dosage. The other test was a lack-of-fit test for the control dose similar to that described above for toxicity effects in the higher doses. The control (zero-dose) data were compared to the linear trend established by the remainder of the data. We refer you to the reference for further details.

EXPERIMENTAL

TEST FUELS

A standard research grade diesel fuel refined by Phillips Chemical Company was chosen as the baseline fuel for this study. This fuel meets the specifications set forth by the EPA in 1993 which was enacted to enforce a 0.05% sulfur (weight) limit on diesel fuel sold in the U.S. The Shell refinery in Bintulu, Malaysia produced the Fischer-Tropsch (FT) fuel. FT fuel is derived from natural gas and contains virtually no sulfur. The physical and chemical specifications of these fuels are given below in Table 1. NETL measurements of density, carbon (wt.%), hydrogen (wt.%) and heat of combustion are also included and reported in parentheses in Table 1. The fuel supplier provided all other data. Heating value, density and carbon (wt.%) and hydrogen (wt.%) are used in engine combustion calculations. Fuel property values measured at NETL and the manufacturer's values were combined and averaged for engine calculations.

Table 1. Fuel Properties

Analysis	Malaysian F-T	Std. Diesel Fuel Phillips Lot D-538)
Density, kg/L @ 15 C	0.7845 (.782)	.8455 (.843)
API Gravity @ 60F (API)	54	35.86
Cetane No.	73.7	46.7
Sulfur Content	<1 ppm	.03 (%)
Heat of Combustion		
Gross Heat Value (BTU/lb)	20273.8 (20264)	(19514)
Net Heat Value (BTU/lb)	18883.5 (18921)	(18322)
Aromatic (% v/v)	0.1	28.3
Saturates (% v/v)	99.8	70.3
Olefins (% v/v)	0.1	1.4
Flash Point (C)	72	69.4
Cloud Point (C)	3	-17.8
Water & Sediment (%)	<0.02	0
Carbon Residue (% mass)	0.02	NR
Ash (% mass)	<0.001	NR
Viscosity (cSt @ 40 C)	3.57	2.54
Corrosion	1A	1A
Pour Point (C)	0	-20.6
Gums & Resins (mg/100 ml)	0.2	NR
Lubricity SDBOCLS (grams)	1700	NR
Lubricity HFRR (micron)	420/540/570	NR
Carbon/Hydrogen (% mass)		
Carbon	84.91 (83.73)	NR (86.74)
Hydrogen	14.94 (14.49)	NR (12.86)
Nitrogen	0.57	NR
Residual	-1.09	NR
Oxygen (by difference)	Negligible	NR

NR (not reported).
( ) Values in parentheses are from measurements made at the National Energy Technology Laboratory (NETL.)

ENGINE TEST BED

The engine facility is located at the U.S. Department of Energy's National Energy Technology Laboratory (NETL) in Morgantown, WV. The NETL engine, a Ricardo Proteus, is a direct injected, two-valve, four-cycle engine with a toroidal combustion bowl in the piston. The engine has a bore and stroke of 130 mm (5.1 in) and 150 mm (6 in) respectively and a swept volume of 1.997 liters (122.4 cu in). The engine has a compression ratio of 13.3:1 and a maximum power output of 55 kW (74 hp) at 36.7 rev/sec (2200 rpm). Startup and engine load is controlled by a 420-volt, 100 hp (75 kW), DC dynamometer. Turbocharger conditions are simulated by using filtered, dried, preheated and pressurized NETL site air source and by using a backpressure control valve in the exhaust. Fuel handling and measurement is accomplished using a gravimetric system. A pump-line-nozzle (PLN) type injection system is used as the fuel delivery system. Additional discussions on the detail of the engine test bed are presented elsewhere [10]. A schematic depicting the general layout and instrumentation of the engine test bed is given in Figure 1.

The Code of Federal Regulations (CFR) 40, Part 86, Subpart N delineates the conceptual design and methodology for dilution tunnel measurement for engine systems operating on diesel fuel. The dilution tunnels are either primary, or primary with secondary dilution. However, other tunnel types, in common use today, offer added convenience or improvement. A partial-flow dilution tunnel is an alternative to full flow dilution tunnel for diluting and sampling diesel engine emissions. Some of the advantages of partial-flow dilution tunnel include smaller size and lower capital cost thereby making them suitable for transportable sampling systems.

In this study a partial flow or "mini-dilution" tunnel was used. The system was designed to sample raw exhaust from the diesel engine exhaust. The system incorporated a small stainless steel tunnel, pump, mass flow and temperature measurement and control instrumentation, and accompanying transfer lines. Dilution air was introduced at one end of the tunnel at four equidistant, circumferentially spaced points. This arrangement assured uniform flow and concentration distribution profiles for the diluted exhaust by the time it reached the sampling probe and sample filter. The dilution tunnel, the pumps, and the mass flow measurement instrumentation were designed for achieving repeatable and accurate dilution ratios of up to 30:1. The dilution ratio was defined as ratio of mass flow rates of raw and diluted exhaust. The total mass flow rate through the dilution tunnel was measured with a mass flow meter. All flow rates measured by mass flow meters were compensated for temperature and pressure effects and expressed in terms of standard conditions. The mass flow meter was protected by a 0.01 micron coalescing filter.

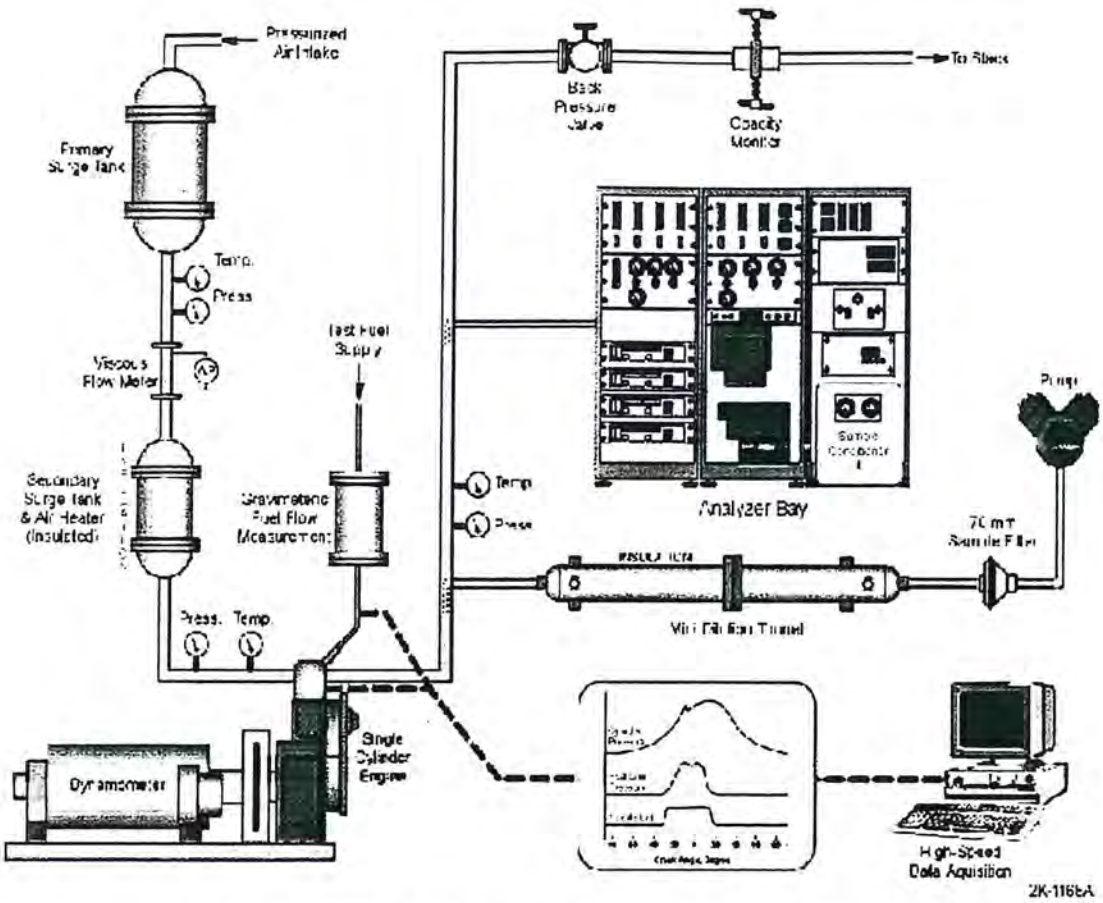

Figure 1. Schematic of Experimental Setup

The amount of sampled engine exhaust was then calculated from the dilution ratio (DR). The dilution ratio is determined from levels of CO_2 in the tunnel (diluted exhaust) and the sampled raw engine exhaust. The total engine exhaust mass sampled was then determined by the mass flow through the tunnel and the dilution ratio.

A constant diluted exhaust flow (DR =12) was maintained throughout the experiments. The dry dilution air was filtered and pressure regulated before passing through a counterflow water to air heat exchanger and air heater to help maintain constant dilution air temperature conditions. The dilution air then flowed through a needle valve for dilution air flowrate control.

The tunnel was designed to satisfy the major criteria for achieving uniform mixing prior to the CO_2 sampling zone and filter. Computational Fluid Dynamic (CFD) modeling was performed which indicated thorough mixing prior to the CO_2 sample probe and filter. The tunnel was well insulated and heated for maintaining constant wall temperature. The inlet to the dilution tunnel consisted of a probe constructed from 3/4" (19 mm) stainless steel tubing which was inserted into the engine exhaust flow. The sampled exhaust then flowed through a short straight section of 1/4" (6.3 mm) well insulated stainless steel flexible transfer pipe. The length of the transfer line was maintained as short as possible and walls well insulated to minimize any sample losses, particularly diffusion and thermophoretic deposition to the tube walls. Sharp bends and other restrictions in the transfer line were avoided.

TEST PROCEDURE

Optimized Thermal Efficiency Timing

A randomized test matrix was derived in order to approach a 95% confidence for the optimum timing conditions for maximum thermal efficiency to be within one crank angle degree (1 °CA) of true optimum. The test involved three replications of 11 independent timing points centered on an estimated optimum. The details of the test design derivation are not provided here for the sake of brevity. The procedure for thermal efficiency injection optimization included setting the fueling to give the required load. The engine emissions were allowed to stabilize and thermal efficiency was recorded. The timing was then set at the next key static timing point. This procedure was repeated allowing the emissions to stabilize at each setting. The time required for stabilization was maintained constant for

each timing change, thus aiding measurement repeatability. Oil and coolant temperatures were kept constant at each key state condition. Thermal efficiency was plotted against static injection timing to establish optimum timing settings for each fuel and key state. The results indicated that optimum timing for the FT fuel and the standard diesel fuels were very similar and effectively equal within the confidence limits. The engine steady state operating conditions or "key states" are given below in Table 2.

Total Particulate Matter (TPM) Sampling

Diesel Particulate Matter (DPM) was collected for mass measurement, extraction and chromatographic analysis at NETL. The extracted SOF was provided to National Institute for Occupational Safety and Health (NIOSH) in Morgantown, WV for Ames bioassay testing.

The DPM was sampled on Pallflex TX40HI20-WW 90-mm Teflon coated glass fiber filters. The filter holder was designed to provide a leak-tight support for the filters and a uniform filter face flow velocity distribution. Filtration efficiency for the Pallflex TX40H120WW has been reported as 92.6-99.99% for particle diameter range of 35-1000 nm [16]. Guerrieri [17], investigated filter face velocity effects on particulate mass from heavy-duty diesel engines and suggested that a filter face velocity range between 40 to 100 cm/sec would exhibit little, if any, influence on collected particulate mass. Flow rates were kept within the range of 35 to 45 cm/sec and dilution ratios were held very near a constant 12:1 ratio for this study.

Prior to exposure, the filters were first extracted in a soxhlet apparatus for 72 hours (600 cycles) to reduce errors in sample weight associated with loss of filter material and then equilibrated in a environmentally controlled chamber at 70 F and 50% relative humidity (RH) for 12 hours. After exposure, the filters were again equilibrated in the constant temperature and relative humidity chamber and weighed to obtain the particulate mass. After weighing, the exposed filters were extracted for 72 hours (approximately 600 cycles) with dichloromethane (DCM) in a Soxhlet apparatus to obtain the soluble organic fraction (SOF). In order to obtain maximum extraction of both high and low molecular weight hydrocarbons for accurate source analysis and bioassay analysis, an extended soxhlet extraction process employing 600 cycles with DCM as the only solvent was chosen for this study. An extended extraction procedure was chosen after reviewing the work of de Lucas [18], Krishna [19], and Montreuil [20] and after considering the need for efficient extraction of SOF for bioassay testing.

MOUDI Samples

The test procedure employed the timing settings given in Table 3. The engine test procedure for collecting size-segregated MOUDI samples was similar to the engine tests in which total particulate filter samples were taken. The test procedure involved identical warm up and shut down before and after each day of testing. The engine load, speed, boost pressure, inlet air conditions were all set. The engine ran at the set condition for 45 minutes allowing oil temperatures etc. to stabilize. During this time the dilution tunnel was turned on allowed to stabilize with respect to dilution ratio, tunnel inlet temperature, dilution air temperature and tunnel wall temperature. When changing fuel, the engine was run until the fueling system was flushed with the new fuel at least two times. The fuel injector nozzles were also checked at the end of each day to ensure integrity.

Table 2. Steady-State Engine Operating Conditions

Key State	Engine Speed (Hz) (rpm/60)	Engine BMEP (bar)	Torque (Nm)	Boost (KpaG)	Inlet Air (C)	Static Timing@	Exhaust (KpaG)
2	16	2	31.8	0	40	11	0
3	16	10	158.9	30	40	13	10
4	24	16	254.3	125	40	17	42
5	24	2	31.8	0	40	10	0
6	32	2	31.8	15	40	16	5
7	32	12	190	160	40	22	53.5
8	24	10	158.9	70	40	15	23.5

@ The same static timing was used for each fuel.

Table 3. Steady-State Operating conditions for MOUDI Sampling

Key State	Engine Speed (Hz) (rpm/60)	Engine BMEP (bar)	Torque (Nm)	Boost (KpaG)	Inlet Air (C)	Static Timing (used for each fuel) °CA	Exhaust (KpaG)
2	16	2	32	0	40	11	0
4	24	16	254	125	40	17	42

For each engine test (sample set consisting of 3 sample replications), separate extractions were performed, on the three combined sets of stages 3 through 8 and on the three combined sets of stages 9, 10 and the afterfilter. After the extraction, the remaining DCM and SOF solution was diluted to 200ml and, as with the total particulate matter samples, 10 ml was taken for later chemical analysis (to determine the Soluble organic fraction (SOF) and the remaining 190 ml was provided to NIOSH for bioassay analysis.

MOUDI Operation

The MOUDI is an inertial 10-stage impactor with each stage or "substrate" collecting particle matter with cutoff diameters as given below in Table 4. At each stage, jets of particle laden gas pass through nozzles accelerating the particles toward the down stream substrate stage. Particles larger than the cut size of the stage cross the air streamlines and are collected on the impaction substrate. The smaller particles with less inertia follow the streamlines and proceed onto the next stage where the nozzles are smaller, the velocity through the nozzles are higher and a smaller cut size of particles are collected. This is continued through the MOUDI cascade impactor until the smallest particles are finally collected at the afterfilter.

The substrates are greased "light," "medium," or "heavy." Stages 0, 1, and 2 were coated with a heavy grease with nominal grease mass between 5.0 and 6.0 mg. Stages 4, 5, and 6 were greased to approximately 3 mg (medium) and stages 7 through 10m were greased at approximately 1.5 mg each (light). The grease (dimethlpolysiloxane, GE product VISC-100M)) was checked for mutagenicity by first applying a known amount of grease on a substrate, then extracting the grease using the standard soxhlet process followed by the Ames bioassay. The results indicated no mutagenic activity (activity was no higher than the background level). This result allowed us to use the greased substrates in lieu of ungreased substrates to ensure high particle capture efficiency with no "particle bounce" [21].

In our procedure, the measured mass size distributions obtained on the MOUDI substrates are expressed in a log-normal form dM/d(log D). The mass distribution is then fitted to a bimodal distribution, via the method of Xu et. al (2002), with each mode being log-normal as given by:

$$\frac{dM}{d(\log D)} = \sum_{j=1}^{n} \frac{M_j}{\log\sigma_j\sqrt{2\pi}} \exp\left[\frac{\left(\log D - \log MMAD_j\right)^2}{-2\log^2\sigma_j}\right] \quad (1)$$

Where D is the aerodynamic particle diameter, M_j is the mass fraction of particles for mode j (substrate j), MMADj is the mass median aerodynamic diameter of the distribution and σ_j is the distribution's geometric standard deviation.

A 30 liter/min sample was drawn through the MOUDI during sampling of the exhaust gases extracted from the mini-dilution tunnel. The MOUDI was calibrated at a 30 liter/min flow by the manufacturer prior to testing. The "as calibrated cut points" values given in Table 4 were determined during the manufacturer's calibration using the same 30 liter/min MOUDI flow rate. Operation, assembly and disassembly, and preparation of the impactor/rotator column was performed in accordance to the procedures outlined in Marple [23].

Measurement and Handling of Filters and Substrates

47 mm aluminum foils (Fisher-Scientific) were used as impaction substrates for size-selective measurements of PM in this study. Thirty-seven millimeter diameter, 0.1 µm pore size filters (Fisher-Scientific) are used as backup filter. The procedures and equipment used for conditioning and weighing filters for total particulate matter gravimetric analysis were also used for treatment and weighing of the substrates and afterfilters designated for size-selective measurements of particulate matter. After exposure, the substrates were again weighed to obtain the particulate mass on each substrate. After re-weighing, the particulate laden substrates were split into three groups. One group was made up of substrates 9, 10 and the after-filter. This group represented the "Ultra-fine particles" or particles with nominal diameters less than 100 nm (0.1 µm). The second group consisted of substrates 3-8. That group represented particles with nominal diameters between 100 nm (0.1 µm) and 3.1 µm. The third group consisted of substrates 0, 1, and 2 and was discarded due to the fact that they contained the most grease per substrate (5 - 6 mg) and because negligible amounts of

Table 4. MOUDI Design and Operation Parameters

Stage	[a]Nominal Cut-Point (μm)	[a]Calibrated Cut-Point (μm)	Nozzle Diameter (cm)	Number of Nozzles	[b]S/W W = nozzle diameter	[c]P/P_o	Nozzle Reynolds No.
Inlet	18	18	1.71	1	0.75	1.00	2420
1	10.0	9.9	0.889	3	0.5	1.00	1560
2	5.6	6.2	0.380	10	1.0	1.00	1090
3	3.2	3.1	0.247	10	1.0	1.00	1680
4	1.8	1.8	0.137	20	1.0	1.00	1510
5	1.0	1.0	0.072	40	1.0	0.99	1440
6	0.56	0.56	0.040	80	1.5	0.97	1340
7	0.32	0.35	0.0140	900	4.1	0.95	350
8	0.18	0.20	0.0090	900	6.4	0.89	580
9	0.10	0.092	0.0055	2000	10.6	0.76	500
10	0.056	0.05	0.0052	2000	11.1	0.53	750

[a] Based on flow rate of 30 l/min at standard atmospheric temperature and pressure.
[b] S = jet to plate distance, W = nozzle diameter.
[c] P = absolute pressure at stage exit with all upstream stages present; P_o = pressure at the MOUDI inlet.

particulate matter were captured. Stages 0, 1, and 2 were therefore not included in the soxhlet extraction and mutagenic studies. The exposed substrates and afterfilters were then extracted for 72 hours (approximately 600 cycles) with dichloromethane (DCM) in a Soxhlet apparatus to obtain the SOF.

Determination of the Soluble Mass for Ames Bioassay dosages

For MOUDI analysis, determination of actual dosages for Ames bioassay analysis had to be determined using a chromatographic technique rather than the standard methods of either evaporating the solute and weighing the remaining solubles or using the difference in mass of the extracted filter and the original filter mass. The reason is that there was no way to retain the particulate material, which was only adhered to the greased surface of the substrate, during the soxhlet extraction process. Further the greased substrates contain an unknown amount of grease, in which a significant part of which remained after the evaporative process.

A chromatographic technique was used to determine the amount of solubles and hence the dosage for the Ames tests. Careful handling and control of the injection process used in the chromatographic analysis allowed accurate determination of sample size. Chromatographic sample size was nominally 2 μl with chromatograms adjusted for slight variations around the nominal. Estimated accuracy of the sample injection was 0.05 μl or 2.5%.

The procedure for calculating the amount of solubles in the MOUDI substrates reduces to a mathematical weighting of the known solubles in a corresponding TPM sample from the same engine operating conditions. The procedure is as follows:

1. First, the total particulate mass on the subject MOUDI substrate sample (W_m) and the corresponding total particulate sample (W_f) collected at the same engine and tunnel operating conditions are determined. The mass of solubles in the total filter sample (W_{fs}) is determined from the difference in the total filter sample mass and the total filter sample mass after soxhlet extraction.
2. Second, determine the area under the chromatogram for the subject MOUDI substrate sample (A_m) and for the corresponding total particulate sample (A_f) collected at the sample engine and tunnel operation conditions per the GC procedure.
3. By proportionally correcting the soluble mass in the total particulate sample (W_{fs}) by the ratio of the GC areas, the estimated weight of solubles in any given MOUDI substrate (W_s sol) is given by:

$$W_s sol = W_{fs} \frac{A_m}{A_f} \qquad (2)$$

4. The solubles are dissolved in 200 ml of DCM. 10 ml is removed for use in the GC analysis. The value of $W_s sol$ accounts for that removal. This is the case for all soxhlet-derived samples.

RESULTS AND ANALYSIS

TOTAL PARTICULATE MATTER (TPM)

Mass Measurements - Total particulate filter samples were taken at the seven steady-state engine operating conditions (key states) given in Table 2. The engine work-specific (brake-specific) total particulate matter (TPM) results are given in Figure 3 for both federal diesel No. 2 (DF) and the Fischer-Tropsch (FT) test fuels. Figure 2 shows some variability in the engine-specific (g/hp-hr) TPM with respect to both fuel type and load. In general, the low-load conditions (key states 2, 5, and 6) show the highest levels of TPM emissions. This is more clearly demonstrated in Figure 3, which gives the average TPM over both fuels at each key state.

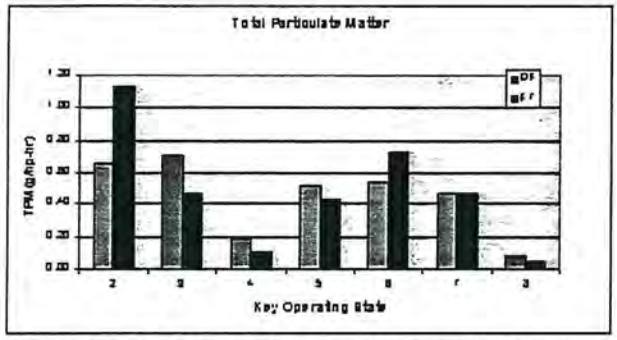

Figure 2. Total particulate matter production at each engine operating condition and fuel type.

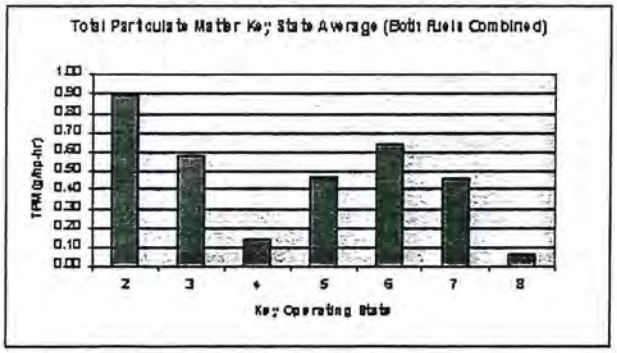

Figure 3. Average total particulate matter production (g/hp-hr) at each engine operating condition.

Key states 4 and 8 (Intermediate-speed high-load and intermediate-speed moderate-load, respectively) demonstrated the lowest TPM. Key state 7, which represents high-speed, 75% load gave about 0.46 g/hp-hr TPM production. Key state 3, which was the low-speed, moderate-load case gave the highest non low-load TPM. These key states were also consistent with regard to the relative difference in TPM between each fuel type.

The low-load conditions (key states 2, 5, and 6) generally produced the highest TPM. This was in part due to lower thermal efficiency at the low load conditions. When those data were presented in purely time-rate units the effect of thermal efficiency were reduced. Total particulate matter production at each key state in grams per hour (g/hr) is given in Figure 4.

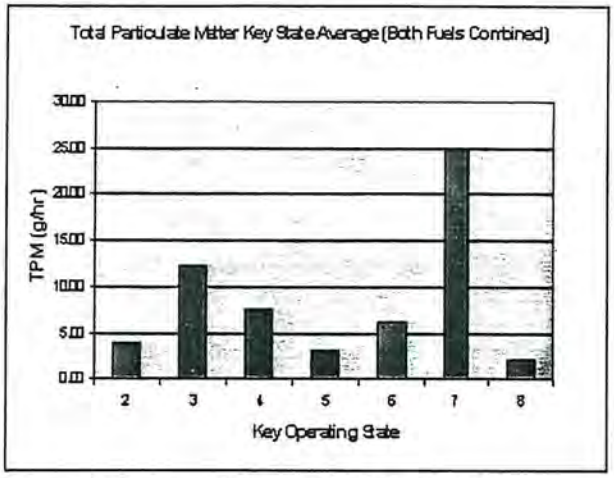

Figure 4. Average total particulate matter production (g/hr) at each engine operating condition.

The test engine, Ricardo Proteous, used a pump-line-nozzle (PLN) type fuel injection system. It was noted in testing that the 90-mm particulate filters from the low-load cases (key states 2, 5 and 6) that the filters obtained a tan colored stain in addition to the dark gray or black particulate matter. This material was later shown to be primarily soluble organics and quite likely originated from partially burned fuel. Fuel injector needle lift was later shown to be incomplete at the low-load cases. This probably led to less than desirable atomization and significant carryover of unburned and partially burned fuel into the exhaust. Poor atomization at low-loads has been demonstrated in early vintage engines employing (PLN) fuel systems. It, in part, was improper low-load atomization and its effect on TPM that drove the development of the modern constant, high-pressure FIE we see today[24].

When considering the differences in TPM with respect to fuel type it can clearly be seen from Figure 2 that the low-load cases influence the overall FT TPM rate by skewing it to the high side. The average TPM from key states 3, 4, 7 and 8 is given in Figure 5. When considering cases other than low-load conditions the relative improvement in TPM reduction from FT fuel is 26% over the DF fuel.

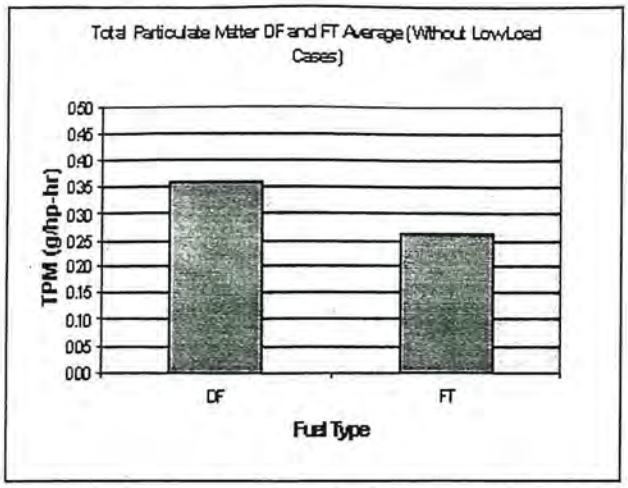

Figure 5. Average total particulate matter (g/hp-hr) for each fuel averaged over key operating states 3,4,7 and 8.

Bioactivity/Comparisons - The mutagenicity (revertants/ug dose) for each fuel type and engine operating conditions is given in Figure 6. Recall that these are averages of the Ames test with 2 bacterial strains both with and without S9 activation. Each of those are the resulting slope of the dose response curve derived from 4 replications of 3-5 dosages. The results and averages at each key state, for each fuel type, bacterial strain and activation are given in Table 5.

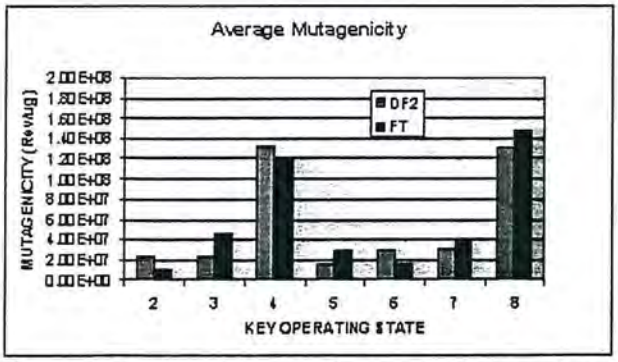

Figure 6. Mutagenicity (Rev/ug) at each operating condition and each fuel type.

The average values given in Table 5 indicate a slight difference in mutagenic activity with regards to fuel type. The FT fuel has on average a 5% greater mutagenic activity (revertants/ug dose). From a practical perspective this difference is slight. These data may also be expressed in engine specific units as well as in time specific units in the same manner as Figures 2 and 4 above. Figures 7 and 8 below give the mutagenicity rate as revertants per hp-hr and revertants per hour. Again, when these data are presented in purely time-rate units (g/hr) the effect of thermal efficiency is reduced. This presentation of the data can be seen as the mutagenic rate potential with operating conditions. In this situation, the FT fuel provides a 45% reduction in revertant rate (rev/hr) over the DF fuel averaged over key states 3, 4, 7 and 8 and 38% over all key states.

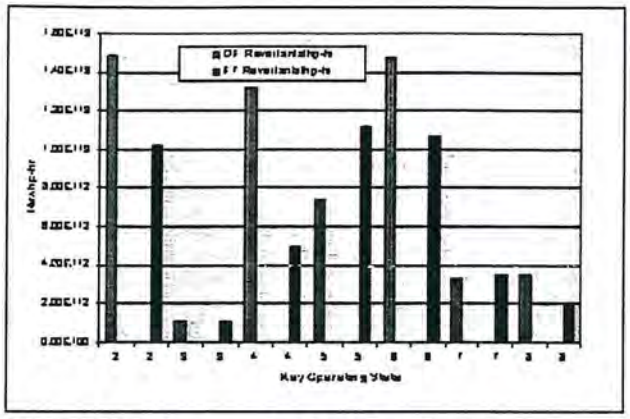

Figure 7. Engine revertant production rate (Revertant/hp-hr) for each key operating state and fuel type.

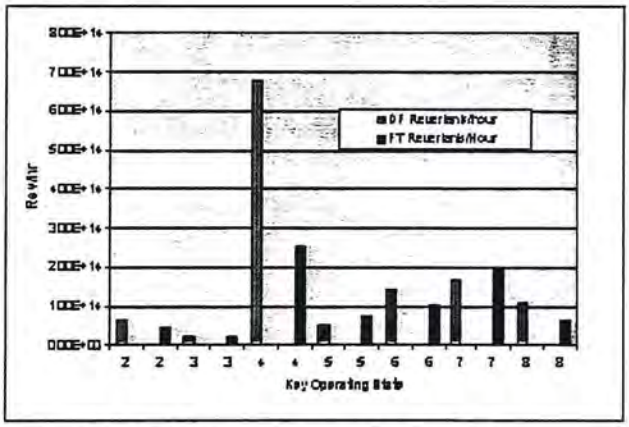

Figure 8. Engine revertant production rate (Revertant/hr) for each key operating state and fuel type.

The result of an analysis of variance (ANOVA) of the mutagenicity data in Table 5 is provided in Table 6. As discussed above, an attempt to remove toxicity effects from the dose response slopes is employed. The highlighted cases in Table 5 represent dose-response slopes that exhibited some degree of remaining toxicity effect. This effect tends to bias the dose-response slope downward thus reducing the apparent exhibited mutagenicity. Again, dosages with toxicity effects are removed until either no toxicity effects remained or 3 dosages remained (i.e. enough to determine a dose-response slope). In any case, toxicity effects are minimized using this method. Also, another test comparing the remaining dose response slope to a zero slope is used to determine a mutagenic threshold (i.e.

Table 5. Mutagenicity (Rev/ug) and averages at each key state, for each fuel type, bacterial strain and activation.*

Key State	DF2				FT				Averages
	YG1024		YG1029		YG1024		YG1029		
	S9-	S9+	S9-	S9+	S9-	S9+	S9-	S9+	
2	4.59E+07	1.76E-07	1.27E+07	3.65E+07	1.70E+07	7.03E+06	2.68E+06	1.06E+07	1.65E+07
3	1.90E+07	3.39E+07	1.68E+07	2.60E+07	3.79E+07	4.84E+07	3.82E+07	5.56E+07	3.45E+07
4	2.31E+08	5.00E+07	1.05E+08	1.42E+08	2.00E+08	4.73E+07	6.41E+07	1.66E+08	1.26E+08
5	2.18E+07	1.01E+07	1.09E+07	1.82E+07	5.08E+07	1.72E+07	1.43E+07	3.22E+07	2.20E+07
6	7.16E+07	2.50E+07	1.30E+07	7.35E+06	2.50E+07	1.30E+07	7.35E+06	1.79E+07	2.25E+07
7	2.66E+07	1.81E+07	2.93E+07	5.19E+07	5.81E+07	1.88E+07	1.70E+07	6.20E+07	3.52E+07
8	3.14E+08	8.46E+07	5.50E+07	6.43E+07	3.70E+08	9.41E+07	5.37E+07	7.57E+07	1.39E+08
	1.04E+08	3.17E+07	3.47E+07	4.94E+07	1.08E+08	3.51E+07	2.82E+07	6.00E+07	
Averages	6.80E+07		4.21E+07		7.18E+07		4.41E+07		
	5.50E+07				5.79E+07				

* The highlights represent dose response slopes in which there was some degree of remaining toxicity effects by the method of Bernstein, et. al; 1982.

Table 6. ANOVA for mutagenicity effects

Summary of Effects (TPM)					
Interaction	SS	DF	MS Effect	F	p-level
Fuel	1.5E+16	1	1.5E+16	10.232	**0.004**
Strain	9.0E+15	1	9.0E+15	6.316	**0.018**
S9	8.0E+15	1	8.0E+15	5.576	**0.026**
Key State	1.3E+17	6	2.1E+16	14.998	**0.000**
Speed	1.8E+14	1	1.8E+14	0.124	0.728
Load	6.0E+16	1	6.0E+16	41.713	**0.000**
Speed x Load	6.8E+15	1	6.8E+15	4.782	**0.038**
$Speed^2$	3.2E+16	1	3.2E+16	22.247	**0.000**
Fuel x Key State	4.2E+15	6	7.0E+14	0.493	0.808
Fuel x Strain	7.4E+13	1	7.4E+13	0.052	0.821
Key State x Strain	3.9E+16	6	6.5E+15	4.555	**0.003**
Fuel x S9	1.4E+14	1	1.4E+14	0.095	0.761
Key State x S9	2.5E+16	6	4.2E+15	2.976	**0.023**
Strain x S9	3.3E+16	1	3.3E+16	23.238	**0.000**

does the dose response differ from the zero control group?). All cases in Table 5 exhibited a positive mutagenic response using this method.

The analysis of variance is based on 2 levels of fuel type (DF and FT), 2 levels each of Salmonella strain and S9 activation and 7 operating conditions (key states). There were 3 levels of engine speed and 4 levels of engine load within the key states. Three-way and higher order interactions are pooled to obtain an error term for testing main effects and two-way interactions. Significant differences between fuel type and key state as well as strain and activation type is indicated. From an interaction perspective, the difference among key states is consistent across fuel types. Within key states the effect speed x load interaction is significant, as is the effect of load in general. There is significant curvature in the speed effect (the quadratic term is significant). The mutagenicity versus engine speed and load is given in Figure 9 using a quadratic response surface fit.

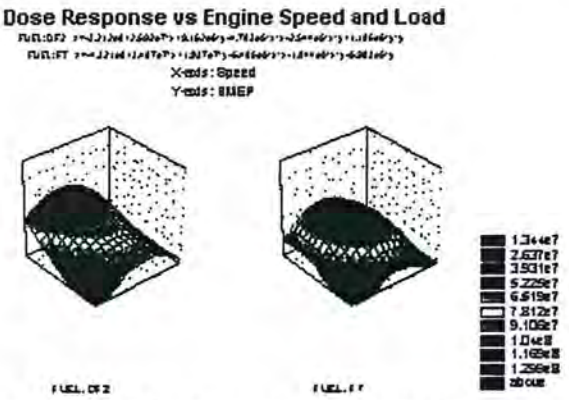

Figure 9. Quadratic response surface of mutagenicity (slope of revertants/ug dose) as a function of engine speed and load.

Greater mutagenic activity can be seen in Figure 9 at intermediate speeds and at higher loads for each fuel type.

SIZE DEPENDENT PARTICULATE MATTER ANALYSIS

Mass Distribution - In our procedure, the measured mass size distributions obtained on the MOUDI substrates are expressed in a log-normal form dM/d(log D). The mass distribution is then fitted to a bimodal distribution, following the method of Xu [22]. Frequency histograms, log-normal frequency curves, the cumulative frequency and cumulative frequency curves are provided for each operating condition and each fuel type. Mass-weighted particulate matter size distributions from MOUDI analysis are given in Figures 10 and 11 for key operating states 2 and 4 respectively.

In Figure 10 (key state 2), both fuel types exhibit most of the mass concentration in region centered near 100 nm with the FT fuel center of mass in the smaller size mode centered at a slightly larger size. The DF fuel exhibits slightly more mass in the coarse mode. In Figure 11 (key state 4), again both fuel types exhibit most of the mass concentration in region centered near 100 nm with the FT fuel center of mass in the smaller size mode centered at a slightly larger size. The DF fuel also has the coarse mode particles centered at a slightly smaller size and a little more of the overall mass is in the larger coarse mode fraction. The relative "split" or center of mass in the near 100 nm particle diameter supports the decision to split the MOUDI substrates into small and large size fractions representing particles above and below 100 nm. By general definition, but not universally established, particles below 100nm are considered ultra-fine particles and those above 100 nm and below 2.5 um are considered fine particles [25].

Bioactivity/Comparisons - For each engine test (sample set consisting of 3 sample replications), separate extractions were performed, on the three combined sets of stages 3 through 8 and on the three combined sets of stages 9, 10 and the afterfilter. After the extraction, the remaining DCM and SOF solution was diluted to 200ml and as with the total particulate matter samples, 10 ml was taken for later chemical analysis (to determine the Soluble organic fraction (SOF)) and the remaining 190 ml was used for bioassay analysis.

The mutagenicity (revertants/ug dose) for each fuel type, engine operating condition and particle size range is given in Figure 12 below. Again, these are averages of the Ames test with 2 bacterial strains both with and without S9 activation. Each of these are the resulting slope of the dose response curve. The groups (2 sm and 4 sm) are made up of substrates 9, 10 and the afterfilter. These groups represents the "Ultra-fine particles" or particles with nominal diameters less than 100 nm (0.1 µm). The second grouping (2 lg and 4 lg) consists of substrates 3-8. This grouping represents particles with nominal diameters between 100 nm (0.1 µm) and 3.1 µm. The results and averages at each key state, for each fuel type, bacterial strain and activation are given in Table 7.

The result of an analysis of variance (ANOVA) of the mutagenicity data in Table 7 is provided in Table 8 using the same methodology as discussed previously. The only case in Table 7 that exhibited a negative mutagenic response for the small particle size of key state 4 for the YG1029 bacterial strain without S9 activation.

The analysis of variance is based on 2 levels of fuel type (DF and FT), 2 levels each of Salmonella strain and S9 activation, 2 size fractions and 2 operating conditions (key states). Significant differences between fuel type, key state and particle size is indicated. Second order interactions between fuel, key state and particle size is indicated.

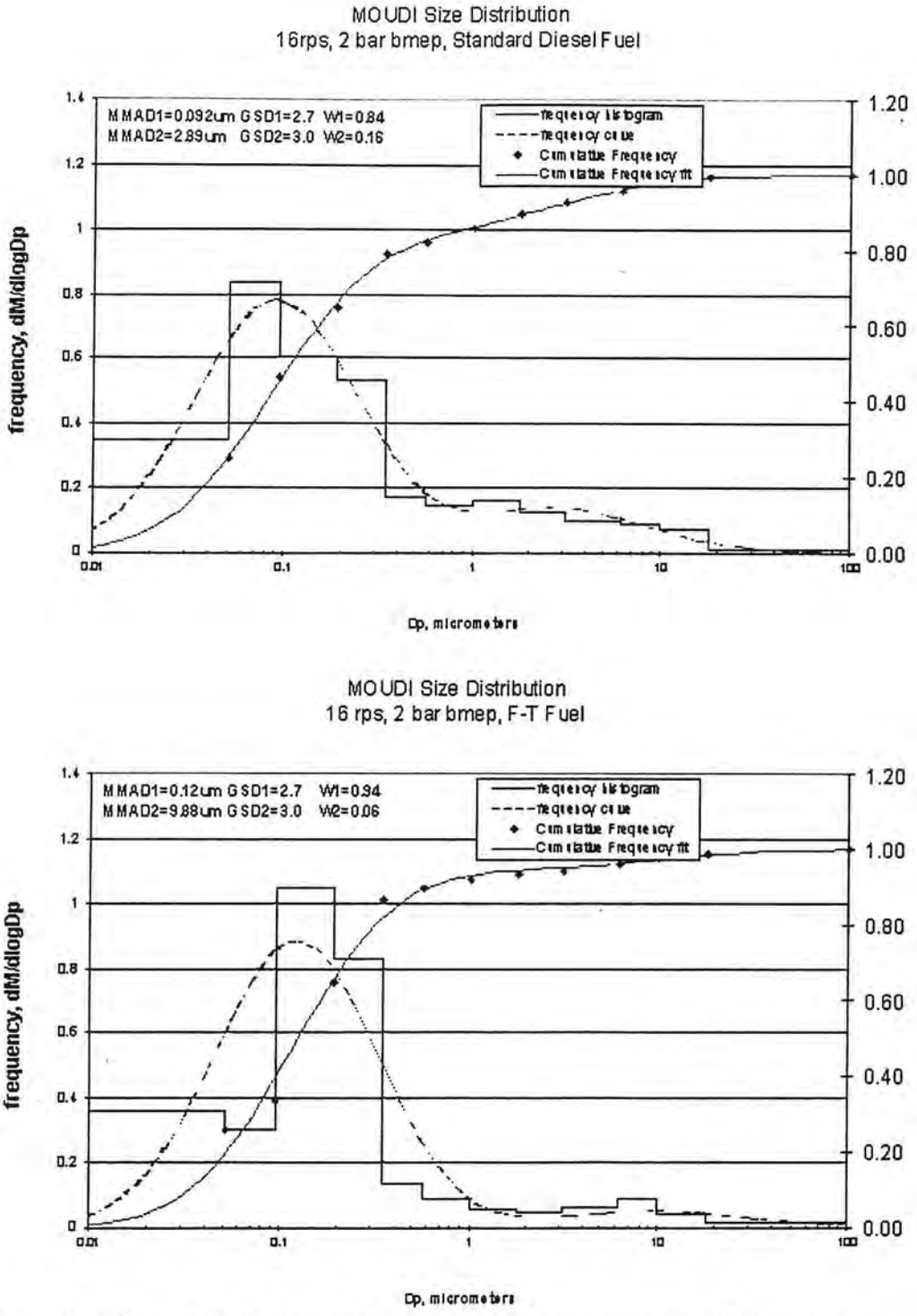

Figure 10. MOUDI size distribution for key state 2 engine conditions (Frequency histograms, log-normal frequency curves, cumulative frequency and cumulative frequency curves)

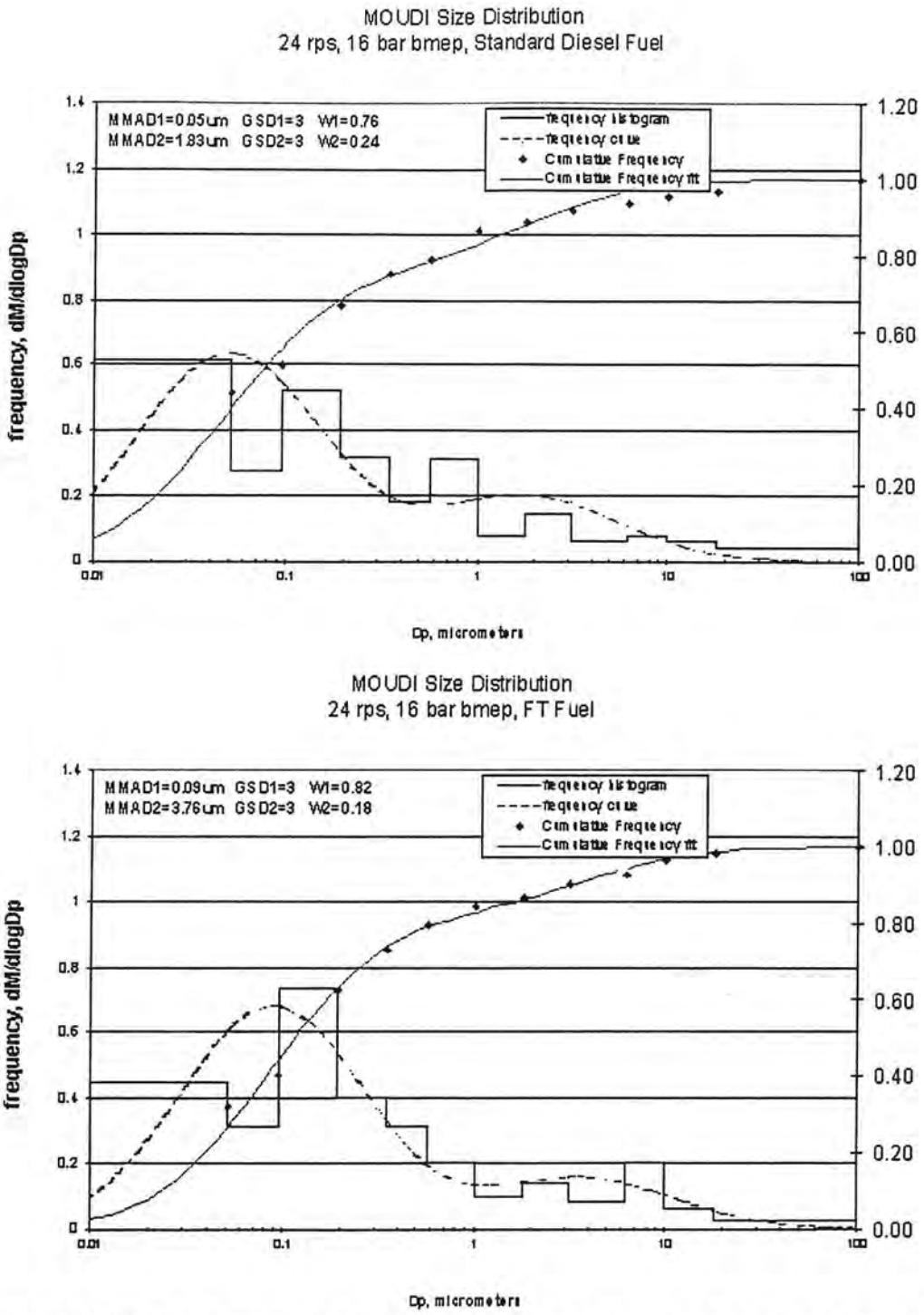

Figure 11. MOUDI size distribution for key state 4 engine operating conditions (Frequency histograms, log-normal frequency curves, cumulative frequency and cumulative frequency curves)

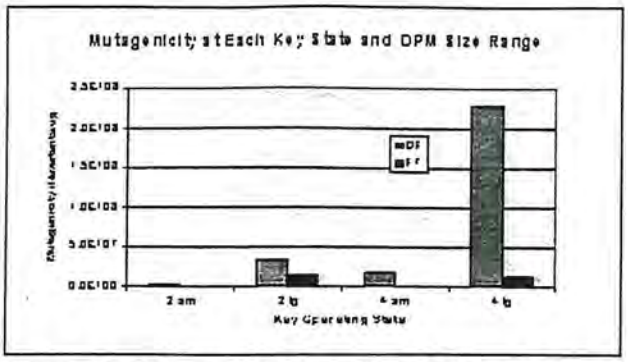

Figure 12. Mutagenicity at each key state, for each fuel type and DPM size range

What separates this analysis from the TPM analysis is the effect of particle size. This effect is significant as indicated by the f ratios and p-levels in Table 8. Larger particles tend to exhibit a significantly larger mutagenic response than smaller size particles. This effect is demonstrated by grouping each fuel as to highlight only key state and size effects as given in Figure 13.

Without weighting for SOF content, the average of the dose response slope at each MOUDI key state qualitatively agrees with the key state averages from the TPM samples. TPM mutagenicity averages for key states 2 and 4 were 1.65 x 10^7 and 1.26 x 10^8 revertants per microgram respectively while the MOUDI averages are 1.28 x 10^7 and 6.5 x 10^7 respectively.

Table 7. Mutagenicity (Rev/ug) and averages at each key state, for each fuel type, bacterial strain and activation for the MOUDI size fractions

Key State/ Size	DF2				FT				Averages
	YG1024		YG1029		YG1024		YG1029		
	S9-	S9+	S9-	S9+	S9-	S9+	S9-	S9+	
2 sm	2.27E+06	2.91E+06	6.74E+05	5.08E+06	1.40E+06	1.40E+06	3.63E+05	2.25E+06	2.04E+06
2 lg	3.47E+07	3.33E+07	1.28E+07	5.23E+07	1.35E+07	1.29E+07	2.86E+06	2.68E+07	2.36E+07
4 sm	2.51E+07	1.75E+07	4.83E+06	2.36E+07	3.08E+05	2.77E+05	7.93E+04	2.12E+05	8.98E+06
4 lg	3.15E+08	2.75E+08	5.85E+07	2.65E+08	1.31E+07	1.43E+07	9.11E+06	1.86E+07	1.21E+08
	9.43E+07	8.23E+07	1.92E+07	8.65E+07	7.06E+06	7.22E+06	3.10E+06	1.20E+07	
Averages	8.83E+07		5.29E+07		7.14E+06		7.53E+06		
	7.06E+07				7.34E+06				

* The highlights represent dose response slopes in which there was some degree of remaining toxicity effects by the method of Bernstein, et. al; 1982.

The mutagenicity versus particle size range and fuel type is given as a scatter plot in Figure 14. The effect of fuel type and particle size is visually demonstrated clearly in the key state 4 plot. The effect, while statistically significant, is less obvious for key state 2 operating conditions. The mutagenicity is not as sensitive to fuel or particle size in key state 2 as it is in key state 4 where it is very responsive to fuel type and size fraction.

CONCLUSIONS

The present effort investigates the mutagenicity of particulate matter derived from FT and DF fuel combustion in a single-cylinder diesel engine by relating the in-vitro mutagenic activity of the particulate to engine operating conditions and particle size using the Ames test. Mutagenicity derived from the Ames test does not necessarily equate to carcinogenicity but it is an important screening tool. Total particulate matter (TPM) filter samples were taken at the seven steady-state engine operating conditions for both federal diesel No. 2 (DF) and the Fischer-Tropsch (FT) test fuels. Particulate matter from two engine conditions are also gathered on greased aluminum foil substrates using a Micro-Orifice Uniform Deposition Impactor (MOUDI) for size selective mutagenic analysis also via the Ames method. Toxicity effects are screened from the dose-response analysis using the method set forth by Bernstein et al, 1982. Specific conclusions are as follows:

- The low-load conditions (key states 2, 5, and 6) generally produced the highest TPM. This is in part due to lower thermal efficiency at the low load conditions and in part due to poor FIE performance at low loads imparting significant carryover of unburned and partially burned fuel and oil components.

Table 8. ANOVA for mutagenicity effects of MOUDI samples

Summary of Effects (MOUDI)				
1-FUEL, 2-KEYSTATE, 3-SIZE, 4-STRAIN, 5-S9				
Interactions	df Effect	MS Effect	F	p-level
1	1	3.2E+16	23.827	0.003
2	1	2.2E+16	16.248	0.007
3	1	3.6E+16	26.651	0.002
4	1	2.5E+15	1.828	0.225
5	1	2.1E+15	1.538	0.261
12	1	2.2E+16	16.684	0.006
13	1	2.3E+16	17.235	0.006
23	1	1.6E+16	12.217	0.013
14	1	2.6E+15	1.911	0.216
24	1	2.5E+15	1.848	0.223
34	1	2E+15	1.482	0.269
15	1	1.1E+15	0.796	0.407
25	1	4.5E+14	0.335	0.584
35	1	1.5E+15	1.132	0.328
45	1	3.9E+15	2.887	0.140

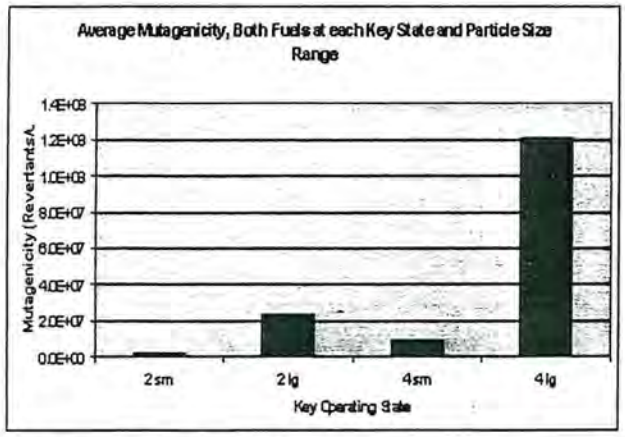

Figure 13. Average mutagenicity each key state and size fraction.

- When considering cases other than low-load conditions the relative reduction in TPM from FT fuel was 26% over the DF fuel.
- When coupled with TPM production rate, the FT fuel provides a 45% reduction in revertant rate (rev/hr) over the DF fuel averaged over key states 3, 4, 7 and 8 and 38% over all operating conditions (key states).

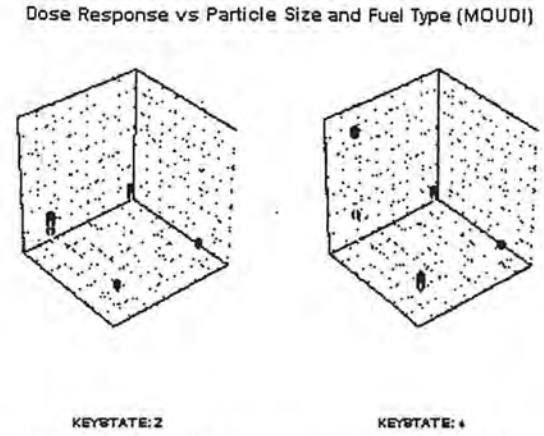

Figure 14. Scatterplot of mutagenicity (slope of revertants/ug dose) as a function of fuel type and particle size for the MOUDI samples.

- The analysis of variance was based on 2 levels of fuel type (DF and FT), 2 levels each of Salmonella strain and S9 activation and 7 operating conditions (key states) using 3 levels of engine speed and 4 levels of engine load within the key states. Significant differences between fuel type and key state as well as strain and activation type is indicated. From an interaction perspective, the difference among key states is consistent across fuel types. Within key states the effect speed x load interaction is significant, as is the effect of load in general. There is significant curvature in the speed effect (the quadratic term is significant).
- Size fractionated MOUDI DPM Ames analysis was performed for 2 size groups at 2 engine conditions. The small size group (2 sm and 4 sm) is made up of substrates 9, 10 and the afterfilter and represents the "Ultra-fine particles" or particles with nominal diameters less than 100 nm (0.1 μm). The second grouping (2 lg and 4 lg) consists of substrates 3-8 and represents particles with nominal diameters between 100 nm (0.1 μm) and 3.1 μm. The measured mass size distributions obtained on the MOUDI substrates, expressed in a log-normal form dM/d(log D) and fitted to a bimodal distribution gave FT fuel mass distributions that were slightly skewed to larger sizes for both MOUDI modes.
- Significant differences in mutagenicity between fuel type, key state and particle size are indicated. Second and third order interactions between fuel, key state and particle size is indicated in the dose response.
- Larger particles tend to exhibit a significantly larger mutagenic response than smaller size particles. This has implications with regard to emissions control as larger particles tend to be more efficiently removed in diesel particulate traps [26]. The remaining smaller

particles may possibly exhibit reduced mutagenicity in regards to their SOF content.

- The mutagenicity is not as sensitive to fuel or particle size in key state 2 as it is in key state 4 where it is very responsive to fuel type and size fraction.

- For all Ames tests (TPM and MOUDI), all but one of 88 dose response slopes were considered to exhibit mutagenic effects.

REFERENCES

1. International Agency for Research on Cancer, "Diesel and Engine Exhausts and Some Nitroarenes, IARC Monographs on the Evaluation of Carcinogenic Risks to Humans," Vol. 46, IARC, Lyon, France, (1989).
2. Bernstein, Leslie, Kaldor, John, McCann, Joyce and Pike, Malcolm C., "An Empirical Approach to the Statistical Analysis of Mutagenesis Data from the Salmonella Test," Mutation Research, 97 267-281 (1982).
3. NIOSH (1988) Current Intelligence Bulletin 50, Carcinogenic Effects of Exposure to Diesel Exhaust. DHHS (NIOSH) Publication No. 88-116. U.S.G.P.O 1988, 548-159:81504.
4. Johansen, K., Gabrielsson, P., Stavnsbjerg, P., Flemming, B., Andersen, E., and Autrup, H., "Effect of Upgraded Diesel Fuels and Oxidation Catalysts on Emission Properties, Especially PAH and Genotoxicity," SAE Paper No. 973001, (1997).
5. Bagley, S.T., Baumgard, K.J., Gratz, L.D., Johnson, J.H., and Leddy, D.G., "Characterization of Fuel and Aftertreatment Device Effects on Diesel Emissions," Health Effects Institute Research Report No. 76, (1996).
6. Ensell, M.X., Whong, W. Z., Heng, Z.C., Nath, J. and Ong, T., "In-vitro and In-vivo Transformation in Rat Tracheal Epithelial Cells Exposed to Diesel Emission Particles and Related Compounds," Mutation Research 412, pp. 283-291, (1998).
7. Nussear, D.L., Gautam, M., Hong-Guang, G., Clark, N., and Wallace, W.E., "Respirable Particulate Genotoxicant Distribution in Diesel Exhaust and Mine Atmospheres, SAE Paper No. 921752, (1992).
8. McMillian, M.H. and Gautam, M., "Consideration for Fischer-Tropsch Derived Liquid Fuels as an Fuel Injection Emission Control Parameter," SAE 982489, (1998).
9. Walsh, Michael P., "Global Trends in Diesel Emissions Regulation - A 2001 Update," SAE 2001-01-0183, (2001).
10. McMillian, M.H. and Gautam, M., "Combustion and Emission Characteristics of Fischer-Tropsch and Standard Diesel Fuel in a Single-Cylinder Diesel Engine," SAE 2001-01-3517, (2001).
11. Schaberg, P.W., Myburgh, I.S., Botha, J.J., Roets, P.N.,Viljoen, C.L., Dancuart, L.P., and Starr, M.E., "Diesel Exhaust Emissions Using Sasol Slurry Phase Distillate Process Fuels," SAE 972898, (1997).
12. Schaberg, P.W., Myburgh, I.S., Botha, J.J. and Khalek, I.A., "Comparative Emissions Performance of Sasol Fischer-Tropsch Fuel in Current and Older Technology Heavy-Duty Engines," SAE 2000-01-1912, (2000).
13. Payri, F., Arregle, J., Fenollosa, C., Belot, G., Delage, A., Schaberg, P., Myburgh, I., and Botha, J., "Characterization of the Injection-Combustion Process in a Common Rail D.I. Diesel Engine Running with Sasol Fischer-Tropsch Fuel," SAE 2000-01-1803, (2000).
14. Maron, D.N., Ames, B.N., "Revised Methods for the Salmonella Mutagenicity Test," Mutation Research 113:173-215, (1983).
15. Wantanabe, M., Ishidate, M. And Nohmi, T., "Sensitive Method for the Detection of Mutagenic Nitroarens and Aromatic Amine: New Derivation of Salmonella typhimurium Tester Strains Possessing Elevated O-acetyltransferase Levels, Mutation Research, 234, 337-348, (1990).
16. Willeke, K. and Baron, P.A., editors Aerosol Measurement: Principles, Techniques and Applications. Van Nostrand Reinhold, New York (1993).
17. Guerrieri, D.A., Rao, V., and Caffery, P.J., "An Investigation of the Effects of Differing Filter Face Velocities on Particulate Mass Weight from Heavy-Duty Diesel Engines," SAE Paper Series 960253 (1996).
18. De Lucas, A., Durán, A, Carmona, M. And Lapuerta, M., "Characterization of soluble Organic Fraction in DPM: Optimization of the Extraction Method," SAE 1999-01-3532, (1999).
19. Krishna, G., Ong, T., Whong, W.Z. and Nath, J., "Mutagenicity Studies of Ambient Airborne Particles: Comparison of Solvent Systems," Mutation Research, 124:113-120, (1983).
20. Montreuil, C.N., Ball, J.C., Gorse, R.A. and Young, W.C., "Solvent Extraction Efficiencies of Mutagenic Components from Diesel Particles," Mutation Research, 282:89-92, (1992).
21. Cheng, Y.S. and Yeh, H.C., Environmental Science and Technology, 13, 1392, (1979).
22. Xu, Z., Gautam, M., and Mehta, S., "Cumulative Frequency Fit for Particle Size Distrubution," Accepted for Publication in the Journal of Applied Occupational and Environmental Hygiene (2002).
23. Marple, V.A., Rubow, K.L., and Behm, S.M., "A Microoriface Uniform Deposit Impactor (MOUDI): Description, Calibration and Use," Aerosol Science and Technology 14:434-446 (1991).
24. Cuenca, R.M., "Evolution of Diesel Fuel Injection Equipment - The Last 20 Years," SAE 933015, (1993).
25. Kittelson, D.B., Arnold, M., and Winthrop, F.W., "Review of Diesel Particulate Matter Sampling Methods - Final Report," University of Minnesota, Minneapolis, MN, (1999).
26. Johnson, T.V., "Diesel Emission Control in Review," SAE 2001-01-0184, (2001).